

# PET Imaging for Gynecologic Malignancies



Saul N. Friedman, MD, PhD<sup>a</sup>, Malak Itani, MD<sup>b</sup>, Farrokh Dehdashti, MD<sup>c,\*</sup>

## KEYWORDS

• PET • Endometrial cancer • Ovarian cancer • Cervical cancer • Vaginal cancer • Vulvar cancer

## KEY POINTS

- 2-Deoxy-2-[<sup>18</sup>F]fluoro-D-glucose (FDG) PET generally has high sensitivity for advanced disease but limited specificity, making it a useful tool for late-stage disease and detecting malignant recurrence, but limiting its role for diagnosis.
- FDG uptake has been correlated with tumor aggressiveness, and can help with treatment planning, particularly of radiation treatment fields.
- Vaginal and vulvar cancers are less common than endometrial, ovarian, and cervical cancers, and investigations on the role of PET are less conclusive and require further studies.
- Many new and emerging PET tracers are promising for evaluating and mapping different receptors, cell proliferation rates, and even hypoxia, helping to direct treatment, but most still require additional testing before they are ready for standard clinical use.

## INTRODUCTION

Approximately 94,000 new cases of gynecologic cancer are diagnosed in the United States each year. Gynecologic cancers are typically separated into 5 groups based on anatomy, listed here from most to least common: endometrium/uterine body, ovary, cervix, vagina, and vulva.<sup>1</sup> Incidence rates are summarized in **Table 1**. These cancers have diverse clinical presentations and prognoses, and their treatment typically includes a combination of radical surgery, chemotherapy, and/or radiotherapy based on the stage of disease.

The stage of disease at diagnosis is predictive of prognosis and is crucial for selection of the best mode of therapy. Gynecologic cancers are typically staged using the International Federation of Gynecology and Obstetrics (FIGO) criteria. Imaging plays an important role in pretreatment evaluation of patients with gynecologic malignancies as well as in the follow-up for response assessment to therapy

and detection of disease recurrence. Imaging of the female pelvis can be achieved using a combination of ultrasonography (US), computed tomography (CT), magnetic resonance (MR) imaging, and PET/CT using 2-deoxy-2-[<sup>18</sup>F]fluoro-D-glucose (FDG) and other emerging radiopharmaceuticals. PET/CT is known to be more accurate than CT or MR imaging alone for staging and can help direct management.<sup>2</sup>

This article discusses the use of FDG-PET/CT and PET/MR for clinical evaluation of the most common types of gynecologic cancers: endometrial, ovarian, cervical, vaginal, and vulvar cancers.

## PET RADIOPHARMACEUTICALS AND IMAGING PROTOCOLS

Anatomic evaluation of gynecologic malignancies is typically performed with a combination of CT and MR imaging.<sup>2-4</sup> PET is commonly coupled with concurrent CT for attenuation correction and

<sup>a</sup> Division of Nuclear Medicine, Edward Mallinckrodt Institute of Radiology, Washington University School of Medicine, 510 South Kingshighway Boulevard, St Louis, MO 63110, USA; <sup>b</sup> Section of Abdominal Imaging, Edward Mallinckrodt Institute of Radiology, Washington University School of Medicine, 510 South Kingshighway Boulevard, St Louis, MO 63110, USA; <sup>c</sup> Division of Nuclear Medicine, Edward Mallinckrodt Institute of Radiology, Alvin J. Siteman Cancer Center, Washington University School of Medicine, 510 South Kingshighway Boulevard, St Louis, MO 63110, USA

\* Corresponding author.

E-mail address: dehdashtif@wustl.edu

**Table 1**  
Incidence of primary gynecologic cancers based on the Centers for Disease Control and Prevention US data from 2012 to 2016<sup>1</sup>

Cancer Location	Incident Cases per 100,000
Uterine body	26.82
Ovary	11.18
Cervix	7.60
Vulvar	2.62
Vaginal	0.66

anatomic localization, which is often of lower resolution than dedicated CT studies and is often performed without contrast. PET/MR imaging is a more recent innovation, but access remains limited to larger institutions and it is not in widespread use. To allow a more in-depth PET review, anatomic evaluation is not the focus of this article. The focus is on FDG because of its widespread clinical use and accepted role in evaluation in malignant diseases. However, it also briefly reviews clinically approved non-FDG radiopharmaceuticals, including somatostatin-receptor and steroid-receptor imaging agents, as well as radiopharmaceuticals that are currently used in research settings that have clinical potential, including human epidermal growth factor receptors (EGFR), DNA-precursor use, and cell hypoxia imaging tracers. The PET tracers discussed here are summarized in **Table 2** along with key procedural parameters.

### Glucose Metabolism

FDG (<sup>18</sup>F: half-life  $T_{1/2}$  = 109.7 minutes), a glucose analogue, is the most common tracer used for clinical evaluation of patients with gynecologic malignancies. The biological basis for the use of FDG in oncology is the Warburg effect, which describes an increase in glycolysis under aerobic conditions and is characteristic of the malignant state. FDG is taken up by the cell using glucose transporters and phosphorylated by hexokinase to FDG-6 phosphate (FDG-6P). FDG-6P is not a good substrate for further metabolism and is trapped within the cell, because glucose 6-phosphatase is markedly downregulated in cancer cells.

Patient preparation for FDG-PET imaging of gynecologic tumors typically follows the Society of Nuclear Medicine and Molecular Imaging guidelines, which includes fasting for at least 4 hours and fasting blood glucose level less than or equal to 200 mg/dL. Typical doses are within 10 to

20 mCi (370–740 MBq). Urinary tract preparation that involves placement of a Foley catheter, intravenous administration of fluids, and furosemide may be performed for evaluation of gynecologic cancers for evaluating lesions close to the bladder. Imaging typically begins 60 minutes after administration of FDG. Standard imaging from the skull base to the thighs typically takes approximately 20 minutes, but depends on patient size and scanner technology. Anatomic imaging protocols differ between institutions and scanners. Although CT oral contrast is used in many centers, the use of intravenous contrast is controversial and limited to some centers. CT images are typically acquired before PET acquisition.

For PET/MR imaging, routine pelvic MR protocols are acquired with and without intravenous contrast, use of antiperistaltic medications, and intravaginal contrast. Acquired sequences differ between institutions, but typically include T1-weighted and T2-weighted sequences, diffusion-weighted imaging, and postcontrast imaging, which enables better evaluation of structures and possible tumor invasion. The use of dynamic contrast-enhanced imaging allows the evaluation of tissue perfusion and oxygenation.<sup>5,6</sup> Although PET/CT enables direct calculation of attenuation correction from the CT data, MR imaging relies on determining tumor composition and associated look-up tables. A common technique relies on Dixon sequences to delineate up to 4 materials within a given pixel, typically background/air, soft tissue, fat, and lung. Limitations include the inability to always properly delineate organs, particularly the lungs, and the inability to accurately identify cortical bone because of insufficient signal, both of which affect the attenuation correction and resulting standardized uptake value (SUV) accuracy.<sup>7,8</sup>

PET analysis is both qualitative and quantitative. Qualitative analysis compares potential malignant uptake with physiologic uptake, including hepatic uptake, blood pool activity, and adjacent organ parenchymal activity. Quantitative uptake most commonly relies on the maximum SUV ( $SUV_{max}$ ) because of ease of measurement, but SUV mean and peak, as well as metabolic tumor volume (MTV) and total lesion glycolysis (TLG), are becoming more accepted.

### Estrogen Receptors

There are 2 types of estrogen receptors (ERs): ER $\alpha$  and ER $\beta$ .<sup>9</sup> <sup>16</sup> $\alpha$ -<sup>18</sup>F-fluoro-17 $\beta$ -estradiol (FES) is an estrogen analogue that was recently approved by US Food and Drug Administration (FDA) for imaging advanced breast cancer and provides imaging

**Table 2**  
PET tracers for evaluation of gynecologic cancers

PET Tracer	Half-Life (T <sub>1/2</sub> )	Typical Dose	Uptake Time	Fasting State
<sup>18</sup> F-FDG	109.7 min	370–740 MBq (10–20 mCi)	60 min	At least 4 h
<sup>68</sup> Ga-DOTATOC	68 min	132–222 MBq (4–6 mCi); should not be <100 MBq	60 min	Not required
<sup>68</sup> Ga-DOTATATE		(2.7 mCi)		
<sup>68</sup> Ga-DOTANOC				
<sup>64</sup> Cu-DOTATATE	12.7 h	148 MBq (4 mCi)	45–90 min	Not required
<sup>18</sup> F-FES	109.7 min	222 MBq (6 mCi); range 111–222 MBq (3–6 mCi)	60 min; range 20–80 min	Not required
<sup>89</sup> Zr-labeled lumretuzumab	3.27 d	37 MBq (1 mCi)	2, 4, and 7 d	Not required
<sup>18</sup> F-FLT	109.7 min	2.6 MBq/kg (0.07 mCi/kg); maximum dose 185 MBq (5 mCi)	60–70 min	Not required
<sup>18</sup> F-FMISO	109.7 min	3.7 MBq/kg (0.1 mCi/kg); maximum 260 MBq (7 mCi)	≥2 h	Not required
<sup>60</sup> Cu-ATSM	23.7 min	481–740 MBq (13–20 mCi)	60-min dynamic imaging and/or static imaging at 30 min	Not required
<sup>64</sup> Cu-ATSM	12.7 h	925 MBq (25 mCi)		

<sup>18</sup>F-FDG, <sup>68</sup>Ga-DOTA-peptides, and <sup>64</sup>Cu-DOTATATE are commonly used in clinical practice, whereas the remaining tracers are mostly investigational.

**Abbreviations:** ATSM, diacetyl-bis(*N*4-ethylthiosemicarbazone); DOTATOC, 1, 4, 7, 10-tetraazacyclododecane- *N*, *N'*, *N''*, *N'''*-tetraacetic acid-D-Phe 1-Tyr 3-octreotide; DOTATATE, 1, 4, 7, 10-tetraazacyclododecane- *N*, *N'*, *N''*, *N'''*-tetraacetic acid-D-Phe 1, Tyr 3-octreotide; DOTANOC, 1, 4, 7, 10-tetraazacyclododecane- *N*, *N'*, *N''*, *N'''*-tetraacetic acid-Nal3-octreotide; FES, 16 $\alpha$ -<sup>18</sup>F-fluoro-17 $\beta$ -estradiol; FLT, 3'-deoxy-3'-[<sup>18</sup>F]fluorothymidine; FMISO, 1-(2'-nitro-1'-imidazolyl)-3-fluoro-2-propranol.

of ERs through selective binding of the ER $\alpha$  isoform.<sup>10,11</sup> However, its use in other cancers, including gynecologic cancers, is limited to research settings under investigational new drug applications. FES is the most investigated steroid-receptor tracer. Typical dose is 6 mCi (222 MBq) with a typical range of 3 to 6 mCi (111–222 MBq). Recommended imaging is 80 minutes (range of 20–80 minutes), but typically investigators use 60 minutes after administration before starting imaging.<sup>10</sup> Fasting is not required.

### Cell Proliferation

3'-Deoxy-3'-[<sup>18</sup>F]fluorothymidine (FLT)<sup>12,13</sup> is a pyrimidine analogue of thymidine, a DNA precursor intended to evaluate cell proliferation rate, but is more a measure of S-phase fraction. Its uptake is via passive diffusion and facilitated transport by type 1 equilibrate nucleoside transporters (ENT1).<sup>14</sup> Although FLT is a specific marker for cell proliferation and a better marker for evaluation of response to therapy than FDG, physiologic uptake of FLT in the bone marrow caused by increased cell proliferation, in the liver secondary to hepatic glucuronidation, and in the urinary tract

as part of the renal clearance of the tracer represent the main limitations of the method.<sup>15</sup> Investigators have used a dose of 0.07 mCi/kg (2.6 MBq/kg), maximum dose of 5 mCi (185 MBq), infused intravenously over 2 minutes, with PET images acquired 60 to 70 minutes after injection for imaging of cervical cancer.<sup>16,17</sup> Patient fasting was not an explicit requirement of the protocol.

### Hypoxia

Tumor hypoxia inhibits radiation therapy by decreasing the availability of oxygen free radicals that cause tumor DNA damage and cell death. Tumor hypoxia also likely limits the efficacy of chemotherapy. Polarographic oxygen sensors are the gold standard of evaluating hypoxia but are limited by the invasive technique and inherent sampling limitations. PET offers a noninvasive means to reliably evaluate the entire tumor and multiple tumor sites at the same time. The PET agents for assessing hypoxia are in 2 groups.<sup>18</sup> The first is fluorine-labeled nitroimidazoles such as 1-(2'-nitro-1'-imidazolyl)-3-fluoro-2-propranol (FMISO)<sup>19</sup>; [<sup>18</sup>F]fluoroazomycin arabinoside (FAZA), a second-generation 2-nitroimidazole; and [<sup>18</sup>F]fluoroerythronitroimidazole

(FETNM), which is more hydrophilic than FMISO. The second group is copper-labeled diacetyl-bis(N4-ethylthiosemicarbazone) (Cu-ATSM) analogues ( $^{60}\text{Cu}$ ,  $T_{1/2} = 23.7$  minutes;  $^{61}\text{Cu}$ ,  $T_{1/2} = 3.32$  hours;  $^{62}\text{Cu}$ ,  $T_{1/2} = 9.7$  minutes; and  $^{64}\text{Cu}$ ,  $T_{1/2} = 12.7$  hours), which have neutral lipophilic molecules with high cell membrane permeability, and are reduced and trapped in hypoxic cells.

A standard dose of FMISO is 0.1 mCi/kg (3.7 MBq/kg) up to a maximum of 7 mCi (260 MBq).<sup>19</sup> A combination of low tumor uptake, slow accumulation in hypoxic tissues, and slow clearance from normoxic tissue caused by the lipophilic nature of the tracer necessitates long wait periods, of 2 hours or more, between injection and imaging.<sup>20</sup>

For  $^{60}\text{Cu}$ -ATSM, a typical dose of 13 to 20 mCi (481–740 MBq) and for  $^{64}\text{Cu}$ -ATSM, a typical dose of 25 mCi (925 MBq) injected intravenously, followed by 60 minutes of dynamic imaging<sup>21,22</sup> or static imaging at 30 minutes after injections, have been reported.<sup>23</sup>

## ENDOMETRIAL CANCER

Approximately 75% to 80% of patients with endometrial cancer are postmenopausal. This disease typically presents with abnormal bleeding resulting in early-stage diagnosis in 75% of patients.<sup>24</sup> The risk factors include abdominal obesity, multiparity, late menopause, smoking, unopposed estrogen therapy, tamoxifen, Lynch syndrome, and diabetes; hormone replacement therapy, although a risk factor, is no longer typically prescribed.<sup>25</sup> There are 2 histologic subtypes: type 1 are well differentiated estrogen-associated endometrioid adenocarcinomas accounting for 75% to 80% and expressing high levels of ERs. Type 2 are aggressive, undifferentiated, estrogen-independent cancers that typically develop in atrophic endometrium and include adenosquamous, serous papillary, clear cell, and undifferentiated types.<sup>25</sup> FIGO staging of endometrial cancer, which was revised in 2009 and is summarized in **Table 3**,<sup>26</sup> does not include an imaging component. However, MR imaging is highly sensitive and specific for revealing important prognostic factors and thus, when available, is recommended as an adjunct to clinical examination.<sup>27,28</sup>

FIGO staging does include involvement of locoregional and distant nodal metastases, which PET can aid in detecting. Nodal metastatic pattern is predominately pelvic, following anterior pelvic, lateral pelvic, hypogastric, and presacral routes, but can then spread to para-aortic lymph nodes<sup>29</sup>; this reflects stage III disease, with para-aortic involvement being more advanced IIIC2 (see **Table 3**). **Fig. 1** shows an example of recurrent

endometrial cancer. More distant nodal spread to abdominal and/or inguinal lymph nodes reflects stage IV disease.<sup>27</sup> **Fig. 2** shows recurrent endometrial adenocarcinoma with distant metastasis.

## FDG-PET

FDG-PET has a limited role in initial staging. Chang and colleagues<sup>30</sup> reported a pooled sensitivity for the detection of pelvic and/or para-aortic metastasis of only 63% based on their meta-analysis, which is insufficient to replace lymphadenectomy. A more recent meta-analysis showed the overall pooled sensitivity, specificity, and area under the curve (AUC) of FDG-PET/CT for detection of lymph node metastases to be 72% (95% confidence interval [CI], 63%–80%), 94% (CI, 93%–96%), and 94% (CI, 85%–99%), respectively, with an overall diagnostic accuracy (Q\* index) of 88%.<sup>31</sup> Most patients with advanced disease also benefit from surgical debulking, and thus the results of FDG-PET are unlikely to deter surgery. However, FDG-PET can play a role in identification of distant metastases and treatment planning, particularly for radiation therapy.<sup>24</sup> Furthermore, greater uterine tumor  $\text{SUV}_{\text{max}}$  has been correlated with greater tumor aggressiveness. In particular, Kitajima and colleagues<sup>32</sup> discovered that patients with  $\text{SUV}_{\text{max}}$  12.7 or greater had a significantly lower disease-free survival rate ( $P = .00042$ ). FDG-PET also has high sensitivity for detection of both local and distant recurrence, ranging from 85.7% to 100%,<sup>33,34</sup> and may therefore be useful for post-therapy surveillance and detection of recurrent disease. In a recent meta-analysis, FDG-PET/CT had an overall pooled sensitivity, specificity, and AUC for detection of endometrial cancer recurrence of 95% (CI, 91%–98%), 91% (CI, 86%–94%), and 97% (CI, 95%–98%), respectively, with overall diagnostic accuracy (Q\* index) of 93%.<sup>31</sup> The National Comprehensive Cancer Network (NCCN) suggests considering FDG-PET/CT if metastasis is suspected at initial staging and for evaluation of suspected recurrence.

## 2-Deoxy-2-[ $^{18}\text{F}$ ]fluoro-D-glucose PET/ Magnetic Resonance

Data on PET/MR are not as extensive as for PET/CT because of its recent clinical adoption. However, in gynecologic as well as nongynecologic malignancies, several investigators<sup>35–37</sup> have already noted that PET/MR is superior to PET/CT in diagnosing brain and liver metastases, as well as removing the diagnostic uncertainty of some abdominal findings; nonetheless, PET/CT remains superior for diagnosing lung metastases. No statistically significant advantage of PET/MR compared

**Table 3**  
**Summary of the revised International Federation of Gynecology and Obstetrics staging of endometrial cancer with adaptation of magnetic resonance findings<sup>27</sup>**

Stage I	Carcinoma confined to the uterus
IA	<50% invasion of the myometrium MR: abnormal signal intensity in endometrial cavity or confined to inner half of myometrium
IB	≥50% invasion of the myometrium MR: extends into the outer half of myometrium
Stage II	Cervical stromal invasion without extension beyond the uterus MR: disruption or focal thinning of cervical stroma
Stage III	Carcinoma spread locally
IIIA	Serosal or adnexal invasion MR: disruption or irregular uterine contour caused by tumor; ovarian nodular tumor
IIIB	Vaginal or parametrial involvement MR: direct tumor extension of upper vagina or/and parametrial tissues
IIIC	Metastasis to pelvic or para-aortic lymph nodes
IIIC1	Metastasis to pelvic lymph node MR: lymph nodes >8 mm in short axis
IIIC2	Metastasis to para-aortic lymph node MR: lymph nodes >10 mm in short axis
Stage IV	Extension to the pelvic wall, lower one-third of the vagina, or hydronephrosis or nonfunctioning kidney
IVA	Bladder or bowel mucosal invasion MR: disruption of bladder or bowel muscular wall with mucosal invasion; not bullous edema
IVB	Distant metastases, including abdominal, or involvement of inguinal lymph nodes MR: tumor deposits at distal sites including peritoneal metastasis, bladder, bone liver metastasis, and distal lymph node metastases

with PET/CT has been ascertained, but data remain limited. Tsuyoshi and colleagues<sup>38</sup> found that non-enhanced PET/MR has similar accuracy to contrast-enhanced CT and that greater SUV/apparent diffusion coefficient (ADC) ratio correlated with high-risk cancers.<sup>39</sup> One of the important advantages of PET/MR, which contributed to the addition of MR, is the evaluation of myometrial invasion because of its high soft tissue resolution.<sup>40</sup> Integrated PET/MR proved significantly more accurate than PET/CT. Bian and colleagues<sup>40</sup> reported an overall detection accuracy of myometrial invasion for PET/CT and integrated PET/MR of 45.9% and 81.8%, respectively ( $P < .001$ ). The depth of myometrial invasion is an important prognostic factor because it strongly correlates with the risk of lymph node metastasis and prognosis in patients with endometrial cancer.<sup>41</sup> Fig. 3 shows an example of FDG-PET/MR and the superiority of MR in evaluation of endometrial cancer.

### **16 $\alpha$ -<sup>18</sup>F-fluoro-17 $\beta$ -estradiol PET**

Endometrial cancer is traditionally divided into estrogen dependent (type 1) and estrogen independent (type 2).<sup>42</sup> The presence of ER $\alpha$  and progesterone receptor in endometrial carcinoma correlates positively with clinical response rate and improved survival, and thus is a potential predictive and prognostic biomarker.<sup>43</sup> Tsujikawa and colleagues<sup>44,45</sup> showed that increasing ratios of FDG/FES uptake can be used as a predictor of not only malignant versus benign tumors but also of malignant aggressiveness and stage. They determined an optimal cutoff ratio of 2.0 resulting in 73% sensitivity, 100% specificity, and 86% accuracy for differentiating malignant from benign lesions, outperforming the 77% accuracy for MR imaging, and noted that a cutoff ratio of 0.5 differentiated carcinoma from hyperplasia with 100% accuracy.<sup>44,45</sup> Results suggest that endometrial carcinoma has a

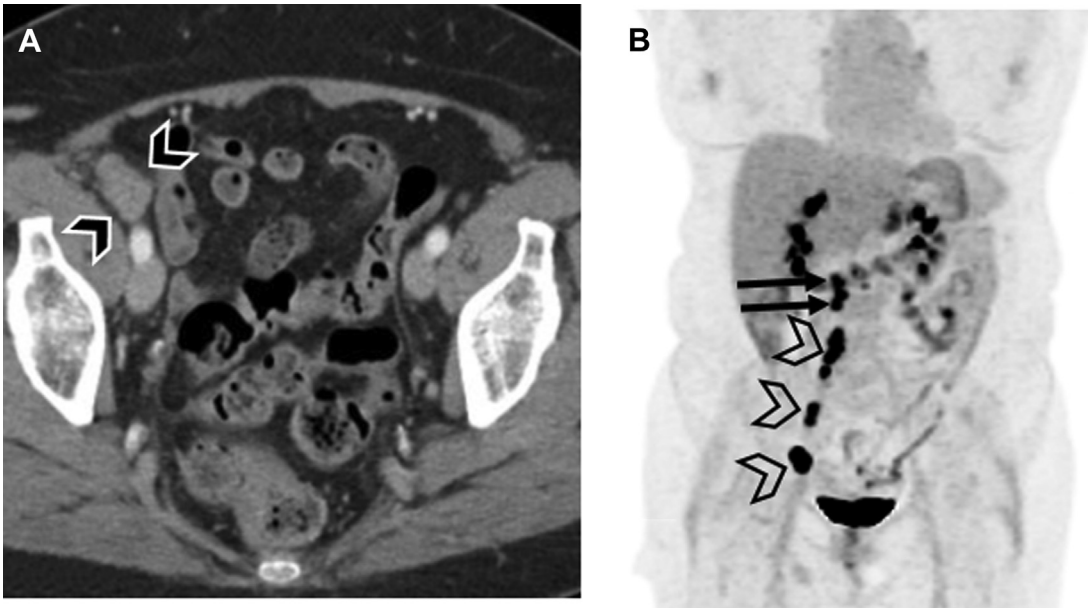


**Fig. 1.** Restaging FDG-PET/CT of a 72-year-old woman with recurrent endometrial malignant mixed müllerian tumor (carcinosarcoma) after hysterectomy, salpingo-oophorectomy, and adjuvant chemotherapy. (A) Axial contrast-enhanced CT image shows a large multilobulated right external iliac lymph node (*arrowheads*). (B) Maximum intensity projection (MIP) image shows markedly hypermetabolic lymphadenopathy along the right external and common iliac chains (*arrowheads*), as well as in the retroperitoneum (*arrows*).

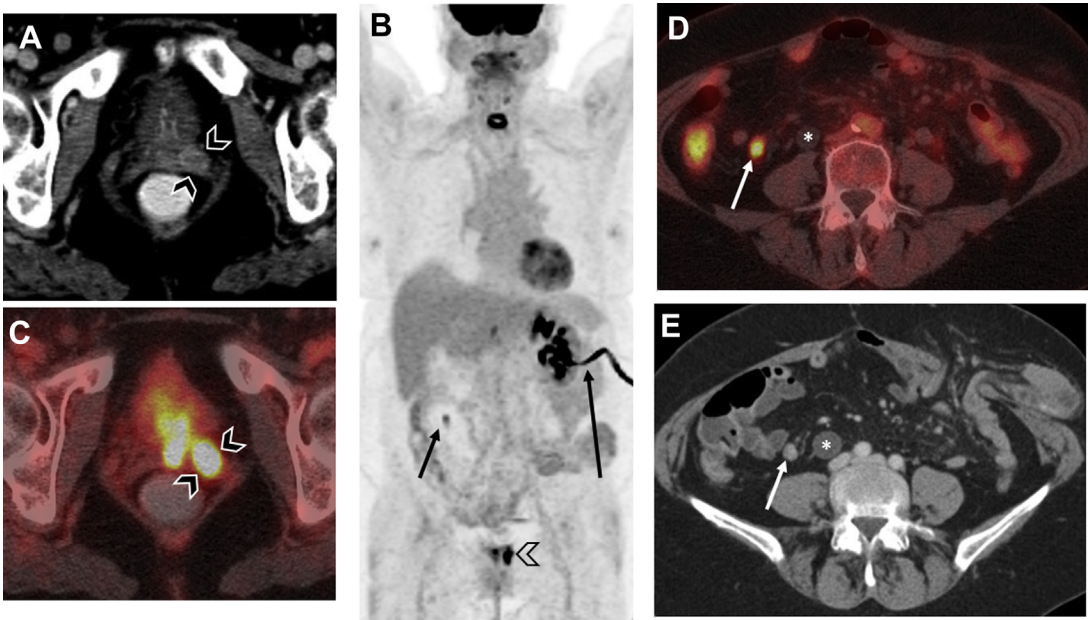


**Fig. 2.** FDG-PET/CT of a 69-year-old woman with recurrent poorly differentiated endometrial adenocarcinoma in the vaginal wall, presenting 13 years after original cancer resection. (A) Axial contrast-enhanced CT image shows an enhancing nodule along the left vaginal wall (*arrowheads*) without additional sites of metastasis. (B, C) PET/CT performed 4 weeks later confirmed a hypermetabolic recurrent left vaginal wall nodule (*arrowheads*) with (D) a metastatic hypermetabolic mesenteric lymph node (*short arrows in B and D*), which retrospectively was present on (E) the prior CT (*arrow*). (D, E) A dilated right ureter caused by a distal ureteral stricture (*asterisks*) and a left nephrostomy tube (*long arrow in B*) are also present.

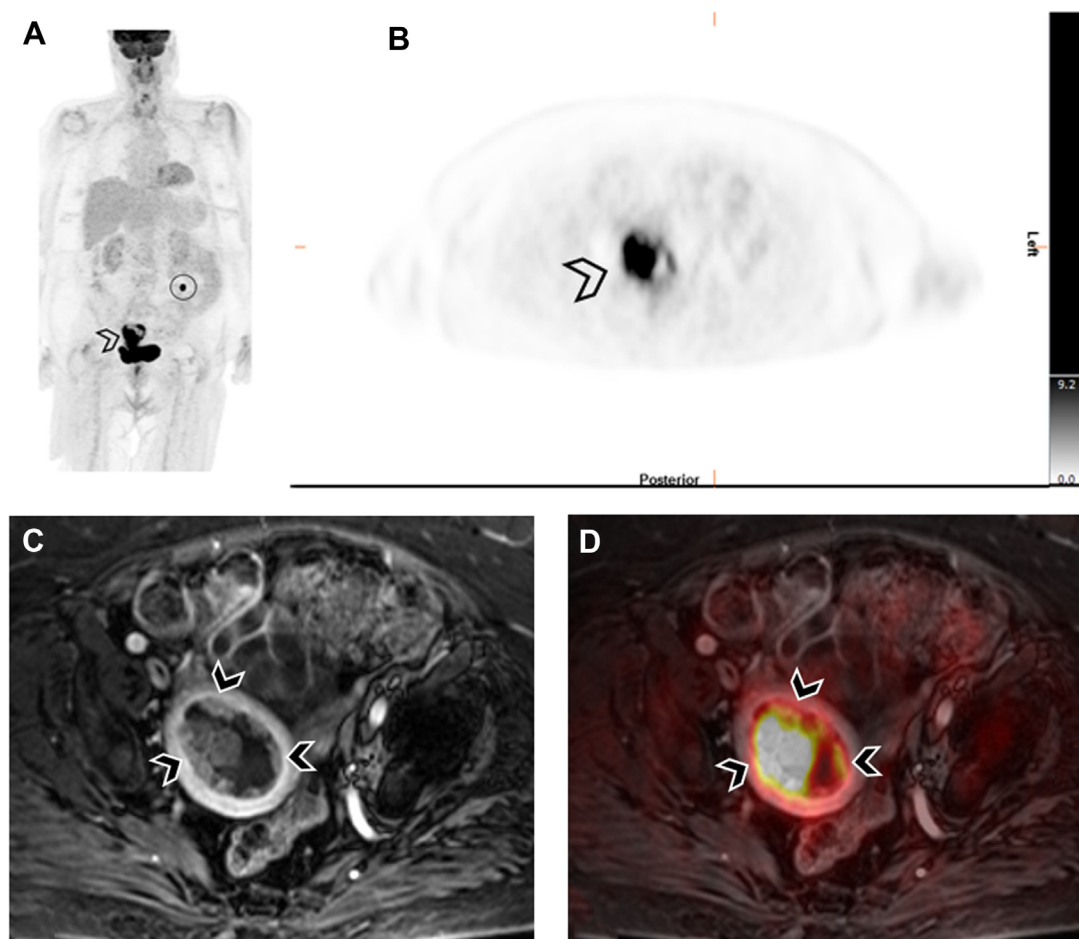


**Fig. 3.** A 64-year-old woman with postmenopausal vaginal bleeding. Pelvic examination showed a bulky cervix with central ulceration, and biopsy was consistent with endometrial endometrioid adenocarcinoma, International Federation of Gynecology and Obstetrics (FIGO) grade II. FDG-PET/MR imaging was performed for initial staging. (A) MIP and (B) axial attenuation-corrected PET images show a markedly hypermetabolic mass (arrowheads) in the endometrial cavity corresponding with a heterogeneously enhancing mass (arrowheads) on (C) axial T1-postcontrast MR imaging and (D) fused images. Incidentally noted was a hypermetabolic focus in the sigmoid colon (circle in A), corresponding with a 3-cm excised tubulovillous adenoma on subsequent colonoscopy.

reduced estrogen dependency and increased glucose metabolism. Zhao and colleagues<sup>46</sup> evaluated FDG and FES as noninvasive biomarkers to assess uterine tumor hormone-receptor expression, glucose metabolism, and proliferation and as a tool to differentiate between uterine leiomyomas and sarcomas. They found a similar relationship of increased FDG/FES ratio in sarcomas compared with leiomyomas of  $5.9 \pm 3.9$  versus  $0.9 \pm 0.5$ , respectively.<sup>46</sup> Now that FES is approved in breast cancer, it is possible that this tracer will be available for evaluating gynecologic cancers in the future.

### 3'-Deoxy-3'-[<sup>18</sup>F]fluorothymidine PET

Uterine leiomyoma is a common benign endometrial tumor, whereas leiomyosarcoma is a rare malignant tumor. However, leiomyomas occasionally

resemble leiomyosarcoma on MR imaging and clinical presentation. Limited data are available for using FLT to distinguish between benign and malignant leiomyomas such as leiomyosarcomas.<sup>47</sup> Yamane and colleagues<sup>47</sup> showed that, although FDG and FLT both had sensitivities and negative predictive values (NPVs) for malignancies of 100%, FLT had better specificity, positive predictive value (PPV), and accuracy of 90.0%, 83.9%, and 93.3% compared with FDG values of 70.0%, 62.5%, and 80.0%, respectively. They also noted that FLT had better correlation with Ki-67 labeling index compared with FDG, with  $R^2 = 0.91$  compared with  $R^2 = 0.26$ . Thus, it is possible that FLT-PET will become a valuable diagnostic tool for differentiating uterine leiomyosarcoma from leiomyoma in the future.

**Table 4**  
**Summary of the revised International Federation of Gynecology and Obstetrics staging of cancer of the ovaries, fallopian tubes, and primary peritoneal cancer<sup>52</sup>**

Stage I	Carcinoma limited to the ovary (or ovaries) or fallopian tubes without spread to nearby lymph nodes or to distant sites	IIIA2	Microscopic extrapelvic (above the pelvic rim) peritoneal involvement with or without positive retroperitoneal lymph nodes
IA	Carcinoma in 1 ovary or 1 fallopian tube, but not on their outer surfaces. No cancer cells in the ascites or washings from the abdomen and pelvis	IIIB	Macroscopic peritoneal metastasis beyond the pelvis up to 2 cm in greatest dimension, with or without metastasis to the retroperitoneal lymph nodes
IB	Carcinoma in both ovaries or fallopian tubes but not on their outer surfaces. No cancer cells in the ascites or washings from the abdomen and pelvis	IIIC	Macroscopic peritoneal metastasis beyond the pelvis more than 2 cm in greatest dimension, with or without metastasis to the retroperitoneal lymph nodes (includes extension of tumor to capsule of liver and spleen without parenchymal involvement of either organ)
IC	Carcinoma in both ovaries or fallopian tubes and any of the following are present:	Stage IV	Carcinoma has spread beyond abdomen and to distant organs
IC1	Surgical spill	IVA	Cancer cells in the pleural fluid
IC2	Capsule ruptured before surgery or tumor on ovarian or fallopian tube surface	IVB	Spread to distant organs
IC3	Cancer cells in the ascites or washings from the abdomen and pelvis		
Stage II	Carcinoma in 1 or both ovaries or fallopian tubes with pelvic extension (below pelvic rim) or primary peritoneal cancer <sup>a</sup> without spread to nearby lymph nodes or to distant sites		
IIA	Extension and/or implants on uterus and/or fallopian tubes and/or ovaries		
IIIB	Extension to other pelvic intraperitoneal tissues		
Stage III	Carcinoma involves 1 or both ovaries or fallopian tubes, or primary peritoneal cancer, with cytologically or histologically confirmed spread to the peritoneum outside the pelvis and/or metastasis to the retroperitoneal lymph nodes without distant metastasis		
IIIA1	Positive retroperitoneal (pelvic and/or para-aortic) lymph nodes only		

<sup>a</sup> There is no stage I peritoneal cancer.

## OVARIAN CANCER

Ovarian cancer is classified into 3 categories based on histology: epithelial, germ cell, and sex cord–stromal tumors. Epithelial ovarian cancer accounts for 95% of ovarian malignancies<sup>48</sup> and originates from the surface epithelial layer of the ovaries or from the distal fallopian tubes.<sup>49</sup> The ovaries are also a common location of metastatic disease, with 5% to 30% of ovarian cancers being metastatic, primarily from the gastrointestinal tract.<sup>50</sup> Early diagnosis is difficult because of the lack of screening and nonspecific symptoms, leading to advanced stage (III or IV) at the time of diagnosis in most patients.<sup>51</sup> Ovarian cancer is surgically staged and, thus, the FIGO staging system for this cancer, summarized in **Table 4**, is surgically based and is defined by the extent and location of disease noted on cytoreduction (ie, debulking) surgery and biopsies.<sup>52</sup>

Ovarian nodal metastatic pattern differs from other gynecologic malignancies because of the embryologic location and subsequent descent. Metastases first spread to retroperitoneal lymph nodes (pelvic and/or para-aortic) representing stage IIIA1.<sup>29</sup> Para-aortic nodal disease typically

first occurs at L1 to L2 level and then spreads retrograde toward the aortic bifurcation. Pelvic pathways follow the ovarian branches of the uterine vessels laterally and extend to external iliac lymph nodes. Mesenteric and inferior phrenic pathways are less common.

### **2-Deoxy-2-[<sup>18</sup>F]fluoro-D-glucose PET**

Benign and physiologic uptake patterns overlap, with physiologic uptake most commonly seen in corpus luteum cysts and endometriomas.<sup>53</sup> Benign ovarian lesions that might show increased FDG uptake also include cystadenomas, teratomas, thecomas, hydrosalpinx, and granulation tissue.<sup>53</sup> FDG-PET/CT can play a role in detecting malignant transformation of endometriomas, because they tend to have higher SUV, with an SUV<sub>max</sub> of 4.0 being suggested as a cutoff.<sup>54</sup>

Epithelial ovarian cancers show variable degree of FDG uptake, and the SUV<sub>max</sub> correlates positively with chemosensitivity and with Ki-67 index,<sup>55</sup> which is likely a macroscopic reflection of the positive correlation between GLUT-1 (glucose transporter 1) expression and tumor proliferation.<sup>56</sup> Although GLUT-1 overexpression is associated with epithelial malignancy, the prognostic value of SUV for FDG is not well established.<sup>56,57</sup> Patient survival is directly linked to successful surgical resection of all malignancy, with unsuccessful debulking and residual tumor greater than 1 cm resulting in increased morbidity without associated survival benefit.<sup>24</sup> FDG-PET/CT in combination with laparoscopy improves detection of disease and increases the likelihood of successful debulking.<sup>58</sup>

FDG-PET/CT performs better than diagnostic CT in preoperative staging, providing 69% concordance with final surgical staging, and 78% concordance when PET is combined with contrast-enhanced CT, compared with 53% by CT alone.<sup>59,60</sup> Fig. 4 shows the greater sensitivity of FDG-PET/CT for showing metastatic deposits compared with the corresponding contrast-enhanced CT in a patient with a high-grade serous carcinoma of the right ovary and peritoneal carcinomatosis at initial staging. Preoperative FDG-PET/CT has been consistently shown to provide high specificity for detecting sites of distant metastatic disease, may alter therapy and direct surgery in patients with advanced disease, and provides a baseline to monitor treatment.<sup>24,61</sup>

FDG-PET has a strong role for monitoring therapy and restaging, and outperforms conventional imaging with reported PPV greater than 90% in the setting of increased cancer antigen (CA) 125

level tumor marker,<sup>62,63</sup> and can also detect disease in symptomatic patients with normal CA-125 levels.<sup>64</sup> An example for FDG-PET detection of recurrent high-grade ovarian serous carcinoma is shown in Fig. 5. FDG-PET/CT confirmed locally recurrent left vaginal cuff disease and identified an additional unsuspected metastatic retroperitoneal lymph node.

### **2-Deoxy-2-[<sup>18</sup>F]fluoro-D-glucose PET/Magnetic Resonance**

Similar to endometrial cancer, PET/MR is not yet officially endorsed for standard-of-care work-up. Although many groups have failed to show a significant difference between PET/MR and PET/CT results, a few groups showed advantages of PET/MR. Fiaschetti and colleagues<sup>65</sup> found FDG-PET/MR to have superior sensitivity, specificity, PPV, and NPV (n = 19) compared with FDG-PET/CT and MR-only imaging, with PET/MR detecting 95% of the malignant lesions (18 out of 19) compared with 74% with PET/CT (14 out of 19). Nakajo and colleagues<sup>66</sup> found that PET/MR, specifically PET/T2-weighting imaging, better localized disease sites compared with PET/CT (n = 31).

### **16 $\alpha$ -<sup>18</sup>F-fluoro-17 $\beta$ -estradiol PET**

Seventy percent of epithelial ovarian cancer is ER $\alpha$  positive,<sup>10</sup> but only 19% of patients show objective response to endocrine therapy, with 51% reporting clinical benefit.<sup>67–69</sup> In patients with epithelial ovarian cancer, van Kruchte and colleagues<sup>10</sup> found a significant correlation between FES uptake and the semiquantitative immunoscore for tumor ER $\alpha$  (r = 0.65, P < .01) based on a sample size of 28 lesions. They proposed a threshold of SUV<sub>max</sub> greater than 1.8 resulting in a 79% sensitivity, 100% specificity, and AUC of 0.86 (95% CI, 0.70–1.00) to distinguish ER $\alpha$ -positive from ER $\alpha$ -negative lesions.<sup>10</sup>

## **CERVICAL CANCER**

Papanicolaou (Pap) screening and human papillomavirus (HPV) vaccination have resulted in the marked reduction of cervical cancer. Pap screening often leads to diagnosis in premalignant or early stage. HPV types 16 and 18 are responsible for approximately 75% of HPV-related cancers. Risk factors include smoking, number of sexual partners, early age of first coitus, diethylstilbestrol exposure, compromised immune system, long-term oral contraceptive use, and HPV infection.<sup>70</sup> Early-stage cancer has a good prognosis of nearly 90% survival at 5 years and is treated

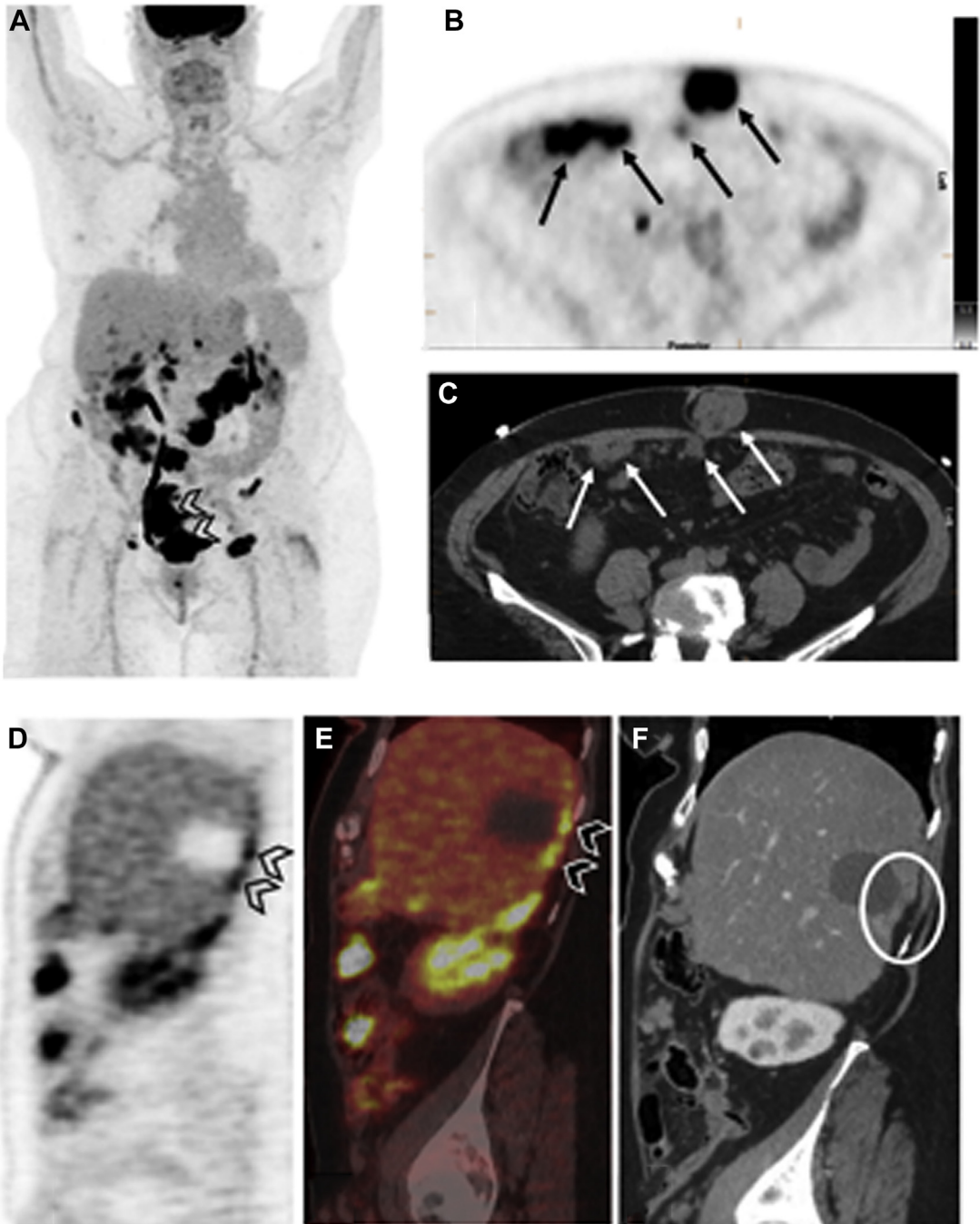


**Fig. 4.** A 77-year-old woman with high-grade serous carcinoma of the right ovary. Initial staging FDG-PET/CT was performed after contrast-enhanced CT of the abdomen and pelvis. (A) MIP PET images show a large hypermetabolic right pelvic primary malignancy (*arrowheads*) and peritoneal carcinomatosis, which is better appreciated on (B) axial attenuation-corrected PET and (C) CT images (*arrows*), extending into an umbilical hernia. Metastatic deposits posterior to the liver (*arrowheads*) can also be visualized on the (D) sagittal PET image and (E) fused PET/CT image. These deposits are harder to appreciate on (F) corresponding sagittal contrast-enhanced CT image (*circle*); the CT scan was performed 10 days after the PET/CT.

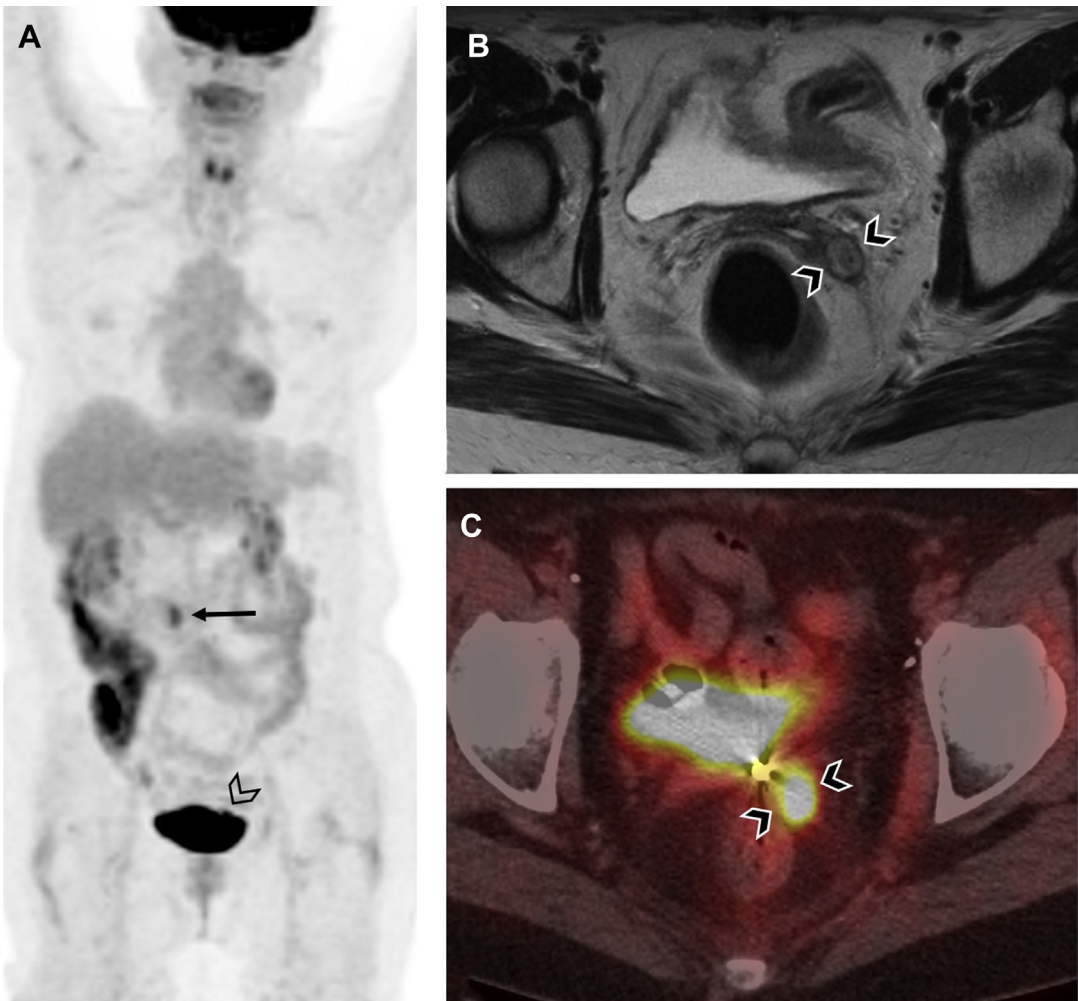


**Fig. 5.** FDG-PET/CT of a 66-year-old woman with recurrent ovarian high-grade serous carcinoma after hysterectomy, salpingo-oophorectomy, and adjuvant intraperitoneal chemotherapy. (A) PET MIP and (B) axial T2-weighted MR imaging show a recurrent nodule in the left vaginal cuff (*arrowheads*). MIP and (C) axial-fused PET/CT images confirm intense hypermetabolic activity within the recurrent left vaginal cuff nodule (*arrowheads*) posterior to the urinary bladder, and an additional metastatic retroperitoneal lymph node (*arrow* on MIP).

with surgical resection, whereas more advanced locally invasive cancers may need definitive chemoradiation. Neoadjuvant therapy is uncommon; advanced stage IV cancer has a 5-year survival rate of only 16%.<sup>24</sup>

Although FIGO staging originally did not incorporate imaging, revised FIGO staging now enables stage IIIC involvement of pelvic and/or para-aortic lymph nodes to be documented by imaging and/or pathology, and is summarized in [Table 5](#),<sup>71</sup> highlighting the importance of nodal status in disease staging. Typical progress of cervical cancer is invasion into the cervical stroma, followed by direct invasion into adjacent parametrium, uterine body, and vagina, and then lymphatic spread. Lymph node metastatic pattern progresses from pelvic

to para-aortic lymph nodes, before distant supraclavicular nodal spread. Hematogenous spread is more typical with advanced disease. An example of an initial staging FDG-PET/CT is presented in [Fig. 6](#), which shows a hypermetabolic primary cervical lesion as well as metastatic left iliac chain lymph nodes; difficulty in assessing local invasion on FDG-PET/CT, requiring MR imaging, is also shown in this example. Prognosis is largely determined by the presence and extent of lymph node involvement, and the presence of metastatic supraclavicular nodes typically indicates an extremely poor prognosis. In patients who undergo surgery, the parametrial surgical margins are also an important prognostic factor.<sup>72</sup>

**Table 5**  
**Revised International Federation of**  
**Gynecology and Obstetrics staging of cervical**  
**cancer, 2018<sup>71</sup>**

Stage I	Carcinoma limited to the uterine cervix
IA	Invasive carcinoma that can be diagnosed only with microscopy, with maximum depth of invasion <5 mm
IA1	Stromal invasion <3 mm in depth
IA2	Stromal invasion $\geq 3$ mm and <5 mm in depth
IB	Invasive carcinoma confined to the uterine cervix, with measured deepest invasion $\geq 5$ mm
IB1 <sup>a</sup>	Tumor measures <2 cm in greatest dimension
IB2 <sup>a</sup>	Tumor measures $\geq 2$ cm and <4 cm in greatest dimension
IB3 <sup>a</sup>	Tumor measures $\geq 4$ cm in greatest dimension
Stage II	Cervical carcinoma invades beyond uterus but not to pelvic wall or to lower third of vagina
IIA	Involvement of the upper two-thirds of the vagina, without parametrial involvement
IIA1	Tumor measures <4 cm in greatest dimension
IIA2	Tumor measures $\geq 4$ cm in greatest dimension
IIB	Parametrial involvement but not up to the pelvic wall
Stage III	Carcinoma extends to pelvic wall, and/or involves lower third of vagina, and/or causes hydronephrosis or nonfunctional kidney, and/or involves para-aortic lymph nodes
IIIA	Involves lower third of vagina, but no extension to pelvic wall
IIIB	Extension to pelvic wall and/or hydronephrosis or nonfunctional kidney from tumor
IIIC <sup>a</sup>	Involvement of pelvic and/or para-aortic lymph nodes, irrespective of tumor size and extent

IIIC1 <sup>a</sup>	Pelvic lymph node metastasis only
IIIC2 <sup>a</sup>	Para-aortic lymph node metastasis
Stage IV	Carcinoma has extended beyond the true pelvis or has involved (biopsy-proven) mucosa of bladder or rectum
IVA	Spread to adjacent pelvic organs
IVB	Spread to distant organs

Uterine sarcomas have a different FIGO staging.

<sup>a</sup> Indicates stages that are new from the 2009 FIGO system. Stage IIIC can be documented by imaging and/or pathology.

### FDG-PET

FDG-PET has a limited role in diagnosis and staging of early cervical cancer, because it suffers from poor sensitivity in the detection of pelvic and para-aortic lymph nodes in early-stage disease; lymphadenectomy is required for disease confirmation and staging, although it is not routinely performed because of its high morbidity.<sup>73,74</sup> Nonetheless, sensitivity of FDG-PET for detection of lymph node metastasis increases with more advanced disease. There are many studies in the literature that evaluated the utility of FDG-PET in cervical cancer. In an early study, Grigsby and colleagues<sup>75</sup> showed that FDG-PET was superior to CT in the detection of abnormal nodes and prediction of treatment outcome. In a later study, they showed that the frequency of FDG-avid lymph nodes correlates with disease stage.<sup>76</sup> Patients with FDG-avid lymph nodes have poorer outcomes compared with patients without FDG-avid lymph nodes within the same stage.<sup>76</sup> A meta-analysis performed by Choi and colleagues<sup>73</sup> showed that FDG-PET/CT significantly outperformed CT and MR imaging with a pooled sensitivity and specificity of 82% and 95%, respectively, with region-based or lymph node-based sensitivity and specificity of 54% and 97%, respectively.

Although FDG-PET may not play a substantial role in disease staging at early stages, it is used to help optimize therapy planning, particularly in radiation therapy planning, and it also provides prognostic information.<sup>77</sup> Pretreatment disease showing greater SUV<sub>max</sub> in the primary or locoregional lymph node metastases is associated with poor outcomes. Pan and colleagues<sup>78</sup> reported that an SUV<sub>max</sub> greater than or equal to 11.2 of the primary tumor significantly ( $P = .0099$ ) predicted worse prognosis. In addition, other FDG parameters of the primary tumor, such as MTV and

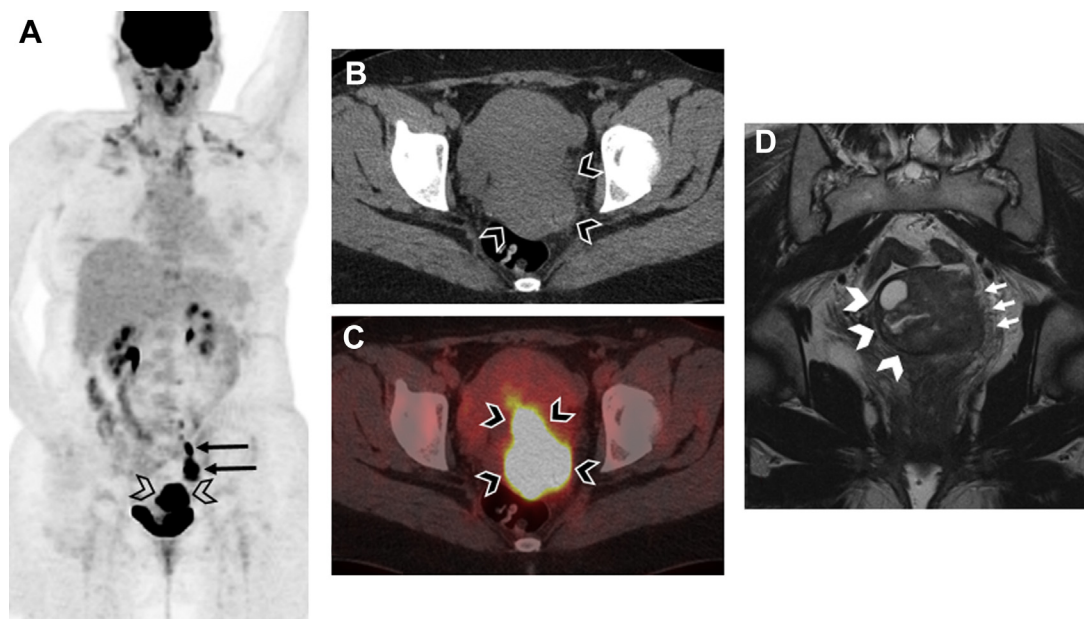


**Fig. 6.** Initial staging FDG-PET/CT of a 39-year-old woman presenting with abnormal vaginal bleeding caused by cervical cancer. Pelvic examination revealed a cervical mass, and biopsy confirmed invasive squamous cell carcinoma. (A) PET MIP, (B) axial CT, and (C) fused axial PET/CT images show a hypermetabolic primary mass in the uterine cervix (*arrowheads*) with metastatic left iliac chain lymph nodes (*arrows*). (D) Coronal T2-weighted MR imaging shows left parametrial invasion, which is hard to appreciate on PET/CT, as shown by infiltrative intermediate signal intensity lines (*short arrows*) causing disruption of the low signal intensity of the left cervical stromal ring compared with the normal right side (*white arrowheads*).

TLG, have been shown to correlate with patient outcome and survival.<sup>79</sup>

FDG-PET also has a role in monitoring therapy response and restaging, with sensitivity ranging between 85% and 100% for recurrent or persistent tumors, including asymptomatic patients.<sup>80,81</sup> Grigsby and colleagues<sup>82</sup> determined that post-treatment abnormal FDG uptake (persistent or new) was the most significant prognostic factor ( $P < .0001$ ) for death from cervical cancer. In a multivariate analysis of prognostic factors, they found a 2-year progression-free survival of 86% for patients without abnormal FDG uptake at any site, but only 40% for those with persistent abnormal uptake. Moreover, there were no survivors at 2 years among patients who developed new sites of abnormal FDG uptake ( $P < .0001$ ).<sup>82</sup> Siva and colleagues<sup>83</sup> had similar findings and calculated a distant failure rate 36-fold lower in patients with complete metabolic response compared with those with only partial response.

### 2-Deoxy-2- $^{18}$ F]fluoro-D-glucose PET/Magnetic Resonance

Although separate MR anatomic imaging and PET/CT both play a role in staging, data on PET/MR remain limited. The investigation of gynecologic malignancies with PET/MR has generally combined endometrial, ovarian, and cervical cancers,

and findings have been generalized across different malignancies. There are a few reports of particular cases where PET/MR changed staging compared with PET/CT. Schwartz and colleagues<sup>84</sup> noted 6 of 18 patients with parametrial invasion and 1 patient with bladder invasion on PET/MR that was not detected on PET/CT. In addition, 5 patients had discordant PET/MR staging compared with clinical staging, of whom 2 patients had management changes because of IIB radiographic staging compared with the original IB1 clinical staging. PET/MR has been shown to have high accuracy in determining T stage and lymph node status in cervical cancer. Grueneisen and colleagues<sup>85</sup> reported that PET/MR imaging was 85% accurate (23 of 27 patients) in determination of the T stage and 93% accurate for nodal detection. Mayerhoefer and colleagues<sup>36</sup> also described change in management of a patient with cervical cancer (9 of 330 patients had gynecologic malignancies) by showing lack of urinary bladder infiltration on PET/MR, which was unclear on the correlating PET/CT, and resulted in the patient receiving both surgery and chemotherapy rather than only chemotherapy. Several studies reported significant associations between PET/MR biomarkers and several prognostic factors, including tumor size, grade, stage, and lymph node metastasis.<sup>85–87</sup> In a recent study, Shih and

colleagues<sup>88</sup> reported that PET/MR biomarkers of cervical cancer are associated with tumor stage and survival;  $SUV_{max}$  and minimum ADC were independent predictors of progression-free survival and overall survival, respectively.

### 3'-Deoxy-3'-[<sup>18</sup>F]fluorothymidine PET

Concurrent use of radiation therapy with chemotherapy is the standard-of-care therapy for most patients with cervical cancers, but increased hematologic toxicity caused by irradiation of physiologic active bone marrow is a common problem.<sup>89,90</sup> FLT-PET has been proposed to identify active bone marrow distribution, enabling tailoring radiation treatment to minimize collateral damage. McGuire and colleagues<sup>16</sup> studied a

combination of patients with cervical and head/neck cancers. They showed that reducing bone marrow radiation dose with the aid of FLT-PET enabled a higher proportion of patients to complete a full course of treatment and reduced bone marrow toxicity.<sup>16</sup> Although FDG can also identify active bone marrow, a small study by Wyss and colleagues<sup>91</sup> showed that FLT had a higher interpatient consistency, and therefore may be the better imaging agent.

### Copper-labeled Diacetyl-bis(N4-ethylthiosemicarbazone) PET

Dehdashti and colleagues<sup>21,22</sup> evaluated pretreatment cervical cancer hypoxia by <sup>60</sup>Cu-ATSM and found an inverse correlation between tracer

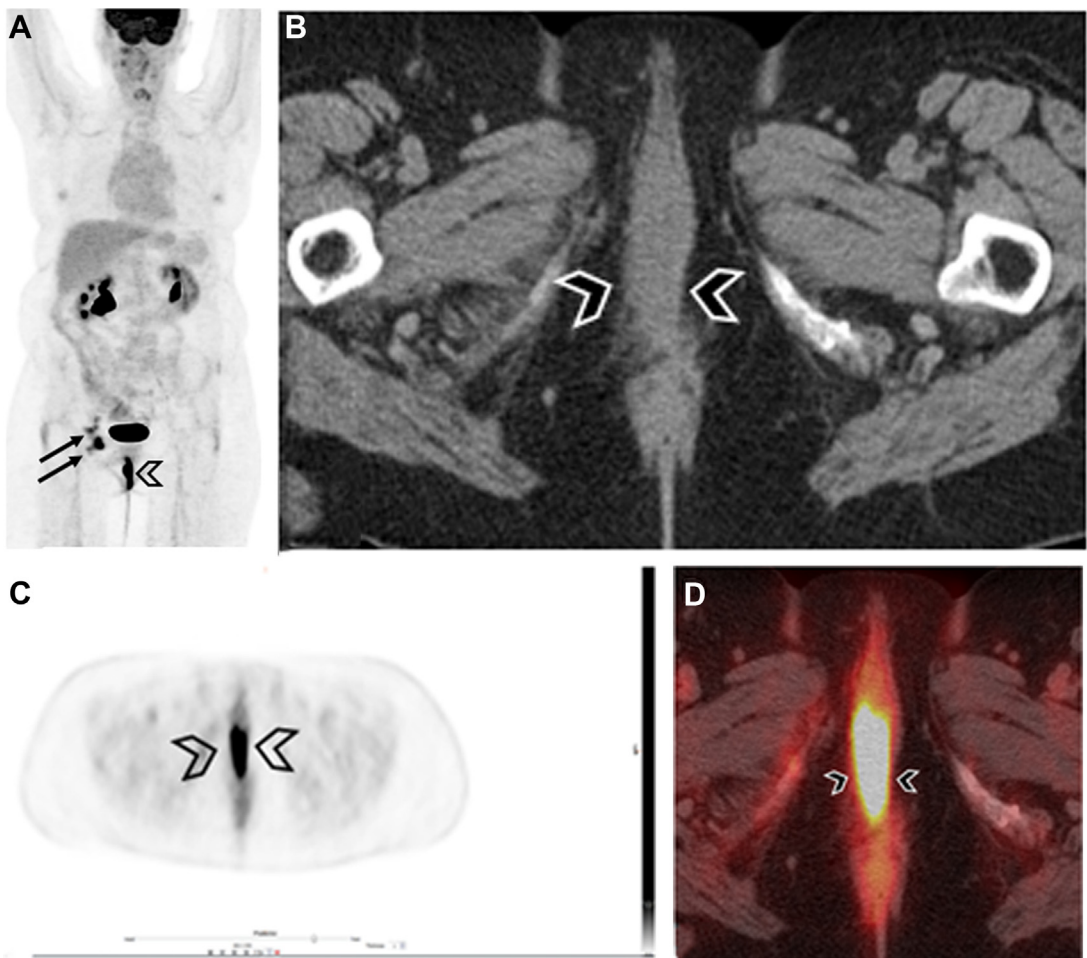


**Fig. 7.** FDG-PET/CT of a 77-year-old woman with recent diagnosis of vulvar squamous cell carcinoma presenting for initial staging. (A) PET MIP image shows a markedly hypermetabolic primary vulvar lesion (arrowhead) with metastatic right inguinal lymph nodes (arrows). (B) Axial CT, (C) axial attenuation-corrected PET, and (D) fused PET/CT images show the primary hypermetabolic carcinoma (arrowheads). Surgical pathology confirmed 7 metastatic right inguinal lymph nodes.

uptake and progression-free survival. A tumor/muscle uptake (T/M) ratio greater than 3.5 correlated with hypoxic tumors, and these patients were likely to develop recurrence with only a 28% 3-year progression-free survival compared with 71% in normoxic tumors with T/M less than or equal to 3.5. However, there was no significant difference between hypoxic and normoxic FDG uptake, and FDG uptake did not correlate with  $^{60}\text{Cu}$ -ATSM uptake.  $^{60}\text{Cu}$ -ATSM uptake has been shown to correlate with FDG-positive lymph nodes and hypoxia-related tumor molecular markers, including vascular endothelial growth factor, cyclooxygenase-2, EGFR, carbonic anhydrase IX (CA-9), and apoptotic index.<sup>92</sup> Subsequent studies comparing  $^{60}\text{Cu}$ -ATSM and  $^{64}\text{Cu}$ -ATSM showed similar findings but lower noise, resulting in better image quality with  $^{64}\text{Cu}$ -ATSM.<sup>23</sup>

## VAGINAL CANCER

Vaginal cancer is rare, representing only 10% of all vaginal malignant neoplasms, and most commonly affects elderly postmenopausal women. Typical presentation is vaginal bleeding or an odorous discharge. Nearly 90% of cases are squamous cell carcinoma, and 8% to 10% of cases are adenocarcinoma. Surgery is limited to early-stage small cancers less than 2 cm, with chemoradiation therapy required for more advanced cases.<sup>93</sup>

Nodal involvement at the time of diagnosis is less common, involving 16% to 40% of cases, but is important because it is associated with worse prognosis and influences management. Vaginal cancer with nodal involvement is typically treated with radiation therapy.<sup>29</sup> Pelvic and inguinal lymph node involvement is considered locoregional disease, with spread via the superficial inguinal pathway, and secondary drainage to the external iliac lymph nodes; confluence of pathways can result in contralateral spread, and laterality is therefore not taken into account for staging.

### 2-Deoxy-2-[ $^{18}\text{F}$ ]fluoro-D-glucose PET

Data on the role of FDG-PET in vaginal cancers are much sparser compared with endometrial, cervical, and ovarian. Lamoreaux and colleagues<sup>94</sup> showed that FDG-PET detects the primary tumor and abnormal lymph nodes more often than diagnostic CT. Robertson and colleagues<sup>95</sup> studied 29 patients with vaginal cancer and found that the physician's prognostic impression changed in 13 of the 29 cases (45%) based on the FDG-PET/CT, 7 patients receiving a better prognosis and 6 receiving a worse prognosis. They also suggested that PET/CT was able to identify abnormalities not

seen on diagnostic CT, but the limited number of patients in the study precludes meaningful statistical analysis.<sup>95</sup> However, the ultimate role of FDG-PET in detecting and monitoring vaginal cancer still requires further studies.

## VULVAR CANCER

Vulvar cancer is rare and often diagnosed in early stages. Squamous cell cancer represents 90% of cases. Risk factors included advanced age, HPV infection, cigarette smoking, inflammatory conditions of the vulva, and immunodeficiency. Standard treatment is radical surgery and sentinel lymph node biopsy with possible inguinofemoral lymphadenectomy.<sup>96</sup>

Nodal metastatic disease is the most important prognostic factor, with 90% survival rate for patients with negative inguinal lymph nodes compared with 50% for those with histologically positive inguinal lymph nodes.<sup>29</sup> One or multiple metastatic nodes, short-axis diameter, and presence of extracapsular spread or ulcerated inguinal adenopathy are all crucial details. As with vaginal cancers, laterality of the locoregional lymph nodes is not considered prognostic.

### 2-Deoxy-2-[ $^{18}\text{F}$ ]fluoro-D-glucose PET

Although data are not as sparse as for vaginal cancer, evaluation of the role of FDG-PET remains much more limited compared with endometrial, cervical, and ovarian cancers. Several studies have suggested that FDG-PET is useful for detecting nodal and distant metastases.<sup>97,98</sup> In particular, Cohn and colleagues<sup>98</sup> reported a sensitivity of 80%, specificity of 90%, PPV of 80%, and NPV of 90% on a patient-by-patient basis. More recently, Kamran and colleagues<sup>99</sup> reported a sensitivity of 50%, specificity of 100%, PPV of 100%, and NPV of 57.1% for detection of lymph node metastases. They concluded that the poor sensitivity makes it unsuitable as a substitute for lymphadenectomy. Similar to their findings on vaginal cancer, Robertson and colleagues<sup>95</sup> found that the physician's prognostic impression changed in 29 of the 54 cases of vulvar cancer (54%). Although ultimately still to be proved, identification of metastatic pelvic nodes on FDG-PET may allow patients to avoid morbidity with unnecessarily extensive surgery in favor of chemoradiation.<sup>100</sup> Investigators such as Lin and colleagues<sup>101</sup> showed that false-positive locoregional and distant metastases on PET are common, and recommended caution with interpretations. **Fig. 7** shows FDG-PET/CT at initial staging of vulvar squamous cell carcinoma with metastatic inguinal lymph nodes.

## FUTURE DIRECTIONS

Several non-FDG tracers have shown promise in evaluating specific phenotypes of gynecologic cancers. These tracers may have a future role in gynecologic imaging. Somatostatin receptor imaging, typically performed with  $^{68}\text{Ga}$ -1, 4, 7, 10-tetraazacyclododecane-*N*, *N'*, *N''*, *N'''*-tetraacetic acid-D-Phe 1-Tyr 3-octreotide (DOTATOC) and  $^{64}\text{Cu}$ -1, 4, 7, 10-tetraazacyclododecane-*N*, *N'*, *N''*, *N'''*-tetraacetic acid-D-Phe 1, Tyr 3-octreotate (DOTATATE), can be used to evaluate rare neuroendocrine variants of cervical and ovarian cancers.<sup>102–106</sup> Vaginal and vulvar human epidermal growth factor receptor (HER) imaging targets HER2 and HER3, using  $^{89}\text{Zr}$ -labeled and  $^{64}\text{Cu}$ -labeled antibodies, is another class of tracers. HER3 overexpression is strongly associated with poor prognosis and could play a role in prediction and monitoring of response to HER3-directed therapy in gynecologic cancers, particularly ovarian cancer.<sup>107,108</sup> Poly(ADP-ribose) polymerase (PARP) inhibitors are an emerging therapeutic class of anticancer drugs with the potential to treat cancers that are deficient in DNA repair machinery.  $^{18}\text{F}$ -FluorThanatrace (FTT), a PARP imaging tracer, is a radiolabeled analogue of the PARP inhibitor rucaparib. FTT is currently in clinical trials in several cancers and has the potential for predicting patient response to PARP-inhibiting therapy, particularly in patients with ovarian cancer.<sup>109,110</sup> FLT, a marker of cell proliferation rate, may be useful in patients with ovarian cancers, identifying malignant lesions and predicting response to therapy.<sup>111–113</sup>

## SUMMARY

Gynecologic cancer staging and management require a multidisciplinary approach with primary oncological and surgical teams working in conjunction with radiology and nuclear medicine physicians to provide patients with optimal care. PET plays a limited role in early-stage disease because this is governed by local disease extent and spread, and is better evaluated with diagnostic CT and MR imaging, and confirmed after possible surgical intervention. FDG-PET plays a role in advanced disease, has been proven to have greater sensitivity compared with CT and MR imaging alone for many of the gynecologic malignancies, and can spare patients unnecessary surgeries. FIGO staging is starting to acknowledge the role and advantage of imaging, and the recent update for cervical cancer now allows for upstaging of cervical cancer based on radiologic identification of pelvic and/or para-aortic lymph node disease.

FDG-PET/MR remains an emerging technology with data currently insufficient to show superiority compared with PET/CT, but several reports suggest superior information of PET/MR on local spread compared with FDG-PET/CT, ultimately leading to change in management. DOTATATE-PET/CT can be a useful tool in mapping disease of rare gynecologic neuroendocrine malignancies of the cervix and ovaries. A brief introduction of other emerging PET tracers is also provided, and although many of these tracers show promise for specialized cancer imaging and characterization, they are currently only used in research settings. Additional studies and data are required to confirm their utility and role in clinical management.

## CLINICAL CARE POINTS

- FDG-PET/CT has a limited role in initial staging of gynecologic cancers and is insufficient to replace lymphadenectomy.
- FDG-PET/CT can play a role in identification of distant metastases and treatment planning for gynecologic cancers.
- $\text{SUV}_{\text{max}}$  has been correlated with greater endometrial tumor aggressiveness.
- No statistically significant advantage of PET/MR compared with PET/CT has been ascertained, but data remain limited.
- PET/CT is superior to PET/MR for detecting lung metastases.
- FDG-PET/MR has superior accuracy for detecting myometrial invasion in endometrial cancer, which is an important prognostic factor.
- Ovarian nodal metastatic pattern differs from other gynecologic malignancies because of their embryology, with metastases first spreading to retroperitoneal lymph nodes (pelvic and/or para-aortic).
- FDG-PET/CT ovarian cancer uptake patterns overlap with physiologic uptake most commonly seen in corpus luteum cysts and endometriomas.
- Ovarian cancer  $\text{SUV}_{\text{max}}$  for FDG correlates positively with chemosensitivity and with Ki-67 index.
- FDG-PET/CT in combination with laparoscopy improves detection of ovarian cancer disease and increases the likelihood of successful debulking.
- FDG-PET/CT performs better than CT in preoperative staging of ovarian cancer.

- FDG-PET/CT outperforms conventional imaging for monitoring therapy and restating of ovarian and cervical cancers.
- Revised cervical cancer FIGO staging now enables stage IIIC involvement of pelvic and/or para-aortic lymph node disease to be documented by imaging and/or pathology.
- FDG-PET/CT sensitivity for metastatic cervical cancer increases with more advanced disease, and outperforms CT and MR imaging in the detection of abnormal nodes and prediction of treatment outcome.
- FDG-avid lymph nodes in cervical cancer correlate with poorer outcomes compared with patients without FDG-avid lymph nodes within the same stage of disease.
- FDG-PET/CT data for vaginal and vulvar cancers are sparse, and more studies are required to determinate its ultimate role.

## DISCLOSURE

The authors have nothing to disclose.

## REFERENCES

1. Center for Disease Control and Prevention. Gynecologic cancer Incidence, United States—2012–2016. USCS data brief, vol. 11. Atlanta, GA: Centers for Disease Control and Prevention: US Department of Health and Human Services; 2019.
2. Alt CD, Brocker KA, Eichbaum M, et al. Imaging of female pelvic malignancies regarding MRI, CT, and PET/CT: Part 2. *Strahlenther Onkol* 2011;187(11):705–14.
3. Brocker KA, Alt CD, Eichbaum M, et al. Imaging of female pelvic malignancies regarding MRI, CT, and PET/CT: part 1. *Strahlenther Onkol* 2011;187(10):611–8.
4. Hricak H. MRI of the female pelvis: a review. *AJR Am J Roentgenol* 1986;146(6):1115–22.
5. Hameeduddin A, Sahdev A. Diffusion-weighted imaging and dynamic contrast-enhanced MRI in assessing response and recurrent disease in gynaecological malignancies. *Cancer Imaging* 2015;15(1):3.
6. Ratner ES, Staib LH, Cross SN, et al. The clinical impact of gynecologic MRI. *AJR Am J Roentgenol* 2015;204(3):674–80.
7. Eiber M, Martinez-Möller A, Souvatzoglou M, et al. Value of a Dixon-based MR/PET attenuation correction sequence for the localization and evaluation of PET-positive lesions. *Eur J Nucl Med Mol Imaging* 2011;38(9):1691–701.
8. Keller SH, Holm S, Hansen AE, et al. Image artifacts from MR-based attenuation correction in clinical, whole-body PET/MRI. *Magma* 2013;26(1):173–81.
9. Gustafsson JA. Estrogen receptor beta—a new dimension in estrogen mechanism of action. *J Endocrinol* 1999;163(3):379–83.
10. van Kruchten M, de Vries EFJ, Arts HJG, et al. Assessment of estrogen receptor expression in epithelial ovarian cancer patients using  $16\alpha$ - $^{18}\text{F}$ -fluoro- $17\beta$ -estradiol PET/CT. *J Nucl Med* 2015;56(1):50–5.
11. Antunes IF, van Waarde A, Dierckx RAJO, et al. Synthesis and Evaluation of the Estrogen Receptor  $\beta$ -Selective Radioligand 2- $^{18}\text{F}$ -Fluoro-6-(6-Hydroxynaphthalen-2-yl)Pyridin-3-ol: Comparison with  $16\alpha$ - $^{18}\text{F}$ -Fluoro- $17\beta$ -Estradiol. *J Nucl Med* 2017;58(4):554–9.
12. McKinley ET, Ayers GD, Smith RA, et al. Limits of [ $^{18}\text{F}$ ]-FLT PET as a biomarker of proliferation in oncology. *PLoS One* 2013;8(3):e58938.
13. Dittmann H, Dohmen BM, Kehlbach R, et al. Early changes in [ $^{18}\text{F}$ ]-FLT uptake after chemotherapy: an experimental study. *Eur J Nucl Med Mol Imaging* 2002;29(11):1462–9.
14. Plotnik DA, Emerick LE, Krohn KA, et al. Different modes of transport for 3H-thymidine, 3H-FLT, and 3H-FMAU in proliferating and nonproliferating human tumor cells. *J Nucl Med* 2010;51(9):1464–71.
15. Shields AF. Positron emission tomography measurement of tumor metabolism and growth: its expanding role in oncology. *Mol Imaging Biol* 2006;8(3):141–50.
16. McGuire SM, Menda Y, Ponto LLB, et al. Spatial mapping of functional pelvic bone marrow using FLT PET. *J Appl Clin Med Phys* 2014;15(4):129–36.
17. Turcotte E, Wiens LW, Grierson JR, et al. Toxicology evaluation of radiotracer doses of 3'-deoxy-3'-[ $^{18}\text{F}$ ] fluorothymidine (18F-FLT) for human PET imaging: Laboratory analysis of serial blood samples and comparison to previously investigated therapeutic FLT doses. *BMC Nucl Med* 2007;7:3.
18. Lopci E, Grassi I, Chiti A, et al. PET radiopharmaceuticals for imaging of tumor hypoxia: a review of the evidence. *Am J Nucl Med Mol Imaging* 2014;4(4):365–84.
19. Lee ST, Scott AM. Hypoxia positron emission tomography imaging with 18f-fluoromisonidazole. *Semin Nucl Med* 2007;37(6):451–61.
20. Koh WJ, Rasey JS, Evans ML, et al. Imaging of hypoxia in human tumors with [ $^{18}\text{F}$ ]fluoromisonidazole. *Int J Radiat Oncol Biol Phys* 1992;22(1):199–212.
21. Dehdashti F, Grigsby PW, Mintun MA, et al. Assessing tumor hypoxia in cervical cancer by positron emission tomography with  $^{60}\text{Cu}$ -ATSM: relationship to therapeutic response—a preliminary report. *Int J Radiat Oncol Biol Phys* 2003;55(5):1233–8.

22. Dehdashti F, Grigsby PW, Lewis JS, et al. Assessing tumor hypoxia in cervical cancer by PET with <sup>60</sup>Cu-labeled diacetyl-bis(N4-methylthiosemicarbazone). *J Nucl Med* 2008;49(2):201–5.
23. Lewis JS, Laforest R, Dehdashti F, et al. An imaging comparison of <sup>64</sup>Cu-ATSM and <sup>60</sup>Cu-ATSM in cancer of the uterine cervix. *J Nucl Med* 2008;49(7):1177–82.
24. Brunetti J. PET/CT in gynecologic malignancies. *Radiol Clin North Am* 2013;51(5):895–911.
25. Cramer DW. The epidemiology of endometrial and ovarian cancer. *Hematol Oncol Clin North Am* 2012;26(1):1–12.
26. Pecorelli S. Revised FIGO staging for carcinoma of the vulva, cervix, and endometrium. *Int J Gynaecol Obstet* 2009;105(2):103–4.
27. Freeman SJ, Aly AM, Kataoka MY, et al. The revised FIGO staging system for uterine malignancies: implications for MR imaging. *Radiographics* 2012;32(6):1805–27.
28. Meissnitzer M, Forstner R. MRI of endometrium cancer - how we do it. *Cancer Imaging* 2016;16:11.
29. Paño B, Sebastià C, Ripoll E, et al. Pathways of lymphatic spread in gynecologic malignancies. *Radiographics* 2015;35(3):916–45.
30. Chang MC, Chen JH, Liang JA, et al. <sup>18</sup>F-FDG PET or PET/CT for detection of metastatic lymph nodes in patients with endometrial cancer: a systematic review and meta-analysis. *Eur J Radiol* 2012;81(11):3511–7.
31. Bollineni VR, Ytre-Hauge S, Bollineni-Balabay O, et al. High Diagnostic Value of <sup>18</sup>F-FDG PET/CT in Endometrial Cancer: Systematic Review and Meta-Analysis of the Literature. *J Nucl Med* 2016;57(6):879–85.
32. Kitajima K, Kita M, Suzuki K, et al. Prognostic significance of SUVmax (maximum standardized uptake value) measured by [<sup>18</sup>F]FDG PET/CT in endometrial cancer. *Eur J Nucl Med Mol Imaging* 2012;39(5):840–5.
33. Ryu SY, Kim K, Kim Y, et al. Detection of recurrence by <sup>18</sup>F-FDG PET in patients with endometrial cancer showing no evidence of disease. *J Korean Med Sci* 2010;25(7):1029–33.
34. Sharma P, Kumar R, Singh H, et al. Role of FDG PET-CT in detecting recurrence in patients with uterine sarcoma: comparison with conventional imaging. *Nucl Med Commun* 2012;33(2):185–90.
35. Martin O, Schaarschmidt BM, Kirchner J, et al. PET/MRI Versus PET/CT for Whole-Body Staging: Results from a Single-Center Observational Study on 1,003 Sequential Examinations. *J Nucl Med* 2020;61(8):1131–6.
36. Mayerhoefer ME, Prosch H, Beer L, et al. PET/MRI versus PET/CT in oncology: a prospective single-center study of 330 examinations focusing on implications for patient management and cost considerations. *Eur J Nucl Med Mol Imaging* 2020;47(1):51–60.
37. Morsing A, Hildebrandt MG, Vilstrup MH, et al. Hybrid PET/MRI in major cancers: a scoping review. *Eur J Nucl Med Mol Imaging* 2019;46(10):2138–51.
38. Tsuyoshi H, Tsujikawa T, Yamada S, et al. Diagnostic value of <sup>18</sup>F-FDG PET/MRI for staging in patients with endometrial cancer. *Cancer Imaging* 2020;20(1):75.
39. Tsuyoshi H, Tsujikawa T, Yamada S, et al. FDG-PET/MRI with high-resolution DWI characterises the distinct phenotypes of endometrial cancer. *Clin Radiol* 2020;75(3):209–15.
40. Bian LH, Wang M, Gong J, et al. Comparison of integrated PET/MRI with PET/CT in evaluation of endometrial cancer: a retrospective analysis of 81 cases. *PeerJ* 2019;7:e7081.
41. Takeuchi M, Matsuzaki K, Harada M. Evaluating Myometrial Invasion in Endometrial Cancer: Comparison of Reduced Field-of-view Diffusion-weighted Imaging and Dynamic Contrast-enhanced MR Imaging. *Magn Reson Med Sci* 2018;17(1):28–34.
42. Bokhman JV. Two pathogenetic types of endometrial carcinoma. *Gynecol Oncol* 1983;15(1):10–7.
43. Singh M, Zaino RJ, Filiaci VJ, et al. Relationship of estrogen and progesterone receptors to clinical outcome in metastatic endometrial carcinoma: a Gynecologic Oncology Group Study. *Gynecol Oncol* 2007;106(2):325–33.
44. Tsujikawa T, Yoshida Y, Kudo T, et al. Functional images reflect aggressiveness of endometrial carcinoma: estrogen receptor expression combined with <sup>18</sup>F-FDG PET. *J Nucl Med* 2009;50(10):1598–604.
45. Tsujikawa T, Yoshida Y, Mori T, et al. Uterine tumors: pathophysiologic imaging with <sup>16</sup>alpha-[<sup>18</sup>F]fluoro-17beta-estradiol and <sup>18</sup>F fluorodeoxyglucose PET—initial experience. *Radiology* 2008;248(2):599–605.
46. Zhao Z, Yoshida Y, Kurokawa T, et al. <sup>18</sup>F-FES and <sup>18</sup>F-FDG PET for differential diagnosis and quantitative evaluation of mesenchymal uterine tumors: correlation with immunohistochemical analysis. *J Nucl Med* 2013;54(4):499–506.
47. Yamane T, Takaoka A, Kita M, et al. <sup>18</sup>F-FLT PET performs better than <sup>18</sup>F-FDG PET in differentiating malignant uterine corpus tumors from benign leiomyoma. *Ann Nucl Med* 2012;26(6):478–84.
48. Desai A, Xu J, Aysola K, et al. Epithelial ovarian cancer: An overview. *World J Transl Med* 2014;3(1):1–8.
49. Erickson BK, Conner MG, Landen CN. The role of the fallopian tube in the origin of ovarian cancer. *Am J Obstet Gynecol* 2013;209(5):409–14.
50. Lee SJ, Bae JH, Lee AW, et al. Clinical characteristics of metastatic tumors to the ovaries. *J Korean Med Sci* 2009;24(1):114–9.

51. Copeland LJ. Epithelial Ovarian Cancer. In: DiSaia PJ, Creasman WT, editors. *Clinical gynecologic oncology*. 7th edition. Philadelphia: Elsevier; 2007. p. 313–67.
52. Prat J, FIGO Committee on Gynecologic Oncology. Staging classification for cancer of the ovary, fallopian tube, and peritoneum. *Int J Gynaecol Obstet* 2014;124(1):1–5.
53. Fenchel S, Grab D, Nuessle K, et al. Asymptomatic adnexal masses: correlation of FDG PET and histopathologic findings. *Radiology* 2002;223(3):780–8.
54. Kusunoki S, Ota T, Kaneda H, et al. Analysis of positron emission tomography/computed tomography in patients to differentiate between malignant transformation of endometrioma and endometrioma. *Int J Clin Oncol* 2016;21(6):1136–41.
55. Liu S, Feng Z, Wen H, et al. 18F-FDG PET/CT can predict chemosensitivity and proliferation of epithelial ovarian cancer via SUVmax value. *Jpn J Radiol* 2018;36(9):544–50.
56. Semaan A, Munkarah AR, Arabi H, et al. Expression of GLUT-1 in epithelial ovarian carcinoma: correlation with tumor cell proliferation, angiogenesis, survival and ability to predict optimal cytoreduction. *Gynecol Oncol* 2011;121(1):181–6.
57. Risum S, Loft A, Høgdall C, et al. Standardized FDG uptake as a prognostic variable and as a predictor of incomplete cytoreduction in primary advanced ovarian cancer. *Acta Oncol* 2011;50(3):415–9.
58. De Iaco P, Musto A, Orazi L, et al. FDG-PET/CT in advanced ovarian cancer staging: value and pitfalls in detecting lesions in different abdominal and pelvic quadrants compared with laparoscopy. *Eur J Radiol* 2011;80(2):e98–103.
59. Castellucci P, Perrone AM, Picchio M, et al. Diagnostic accuracy of 18F-FDG PET/CT in characterizing ovarian lesions and staging ovarian cancer: correlation with transvaginal ultrasonography, computed tomography, and histology. *Nucl Med Commun* 2007;28(8):589–95.
60. Nam EJ, Yun MJ, Oh YT, et al. Diagnosis and staging of primary ovarian cancer: correlation between PET/CT, Doppler US, and CT or MRI. *Gynecol Oncol* 2010;116(3):389–94.
61. Han S, Woo S, Suh CH, et al. Performance of pre-treatment <sup>18</sup>F-fluorodeoxyglucose positron emission tomography/computed tomography for detecting metastasis in ovarian cancer: a systematic review and meta-analysis. *J Gynecol Oncol* 2018;29(6):e98.
62. Palomar A, Nanni C, Castellucci P, et al. Value of FDG PET/CT in patients with treated ovarian cancer and raised CA125 serum levels. *Mol Imaging Biol* 2012;14(1):123–9.
63. Peng NJ, Liou WS, Liu RS, et al. Early detection of recurrent ovarian cancer in patients with low-level increases in serum CA-125 levels by 2-[F-18]fluoro-2-deoxy-D-glucose-positron emission tomography/computed tomography. *Cancer Biother Radiopharm* 2011;26(2):175–81.
64. Bhosale P, Peungjesada S, Wei W, et al. Clinical utility of positron emission tomography/computed tomography in the evaluation of suspected recurrent ovarian cancer in the setting of normal CA-125 levels. *Int J Gynecol Cancer* 2010;20(6):936–44.
65. Fiaschetti V, Calabria F, Crusco S, et al. MR-PET fusion imaging in evaluating adnexal lesions: a preliminary study. *Radiol Med* 2011;116(8):1288–302.
66. Nakajo K, Tatsumi M, Inoue A, et al. Diagnostic performance of fluorodeoxyglucose positron emission tomography/magnetic resonance imaging fusion images of gynecological malignant tumors: comparison with positron emission tomography/computed tomography. *Jpn J Radiol* 2010;28(2):95–100.
67. Hasan J, Ton N, Mullamitha S, et al. Phase II trial of tamoxifen and goserelin in recurrent epithelial ovarian cancer. *Br J Cancer* 2005;93(6):647–51.
68. Bowman A, Gabra H, Langdon SP, et al. CA125 response is associated with estrogen receptor expression in a phase II trial of letrozole in ovarian cancer: identification of an endocrine-sensitive subgroup. *Clin Cancer Res* 2002;8(7):2233–9.
69. Papadimitriou CA, Markaki S, Siapkarakas J, et al. Hormonal therapy with letrozole for relapsed epithelial ovarian cancer. Long-term results of a phase II study. *Oncology* 2004;66(2):112–7.
70. Duarte-Franco E, Franco EL. Cancer of the Uterine Cervix. *BMC Womens Health* 2004;4(Suppl 1):S13.
71. Bhatla N, Berek JS, Cuello Fredes M, et al. Revised FIGO staging for carcinoma of the cervix uteri. *Int J Gynaecol Obstet* 2019;145(1):129–35.
72. Tran BN, Grigsby PW, Dehdashti F, et al. Occult supraclavicular lymph node metastasis identified by FDG-PET in patients with carcinoma of the uterine cervix. *Gynecol Oncol* 2013;90(3):572–6.
73. Choi HJ, Ju W, Myung SK, et al. Diagnostic performance of computer tomography, magnetic resonance imaging, and positron emission tomography or positron emission tomography/computer tomography for detection of metastatic lymph nodes in patients with cervical cancer: meta-analysis. *Cancer Sci* 2010;101(6):1471–9.
74. Ferrandina G, Petrillo M, Restaino G, et al. Can radicality of surgery be safely modulated on the basis of MRI and PET/CT imaging in locally advanced cervical cancer patients administered preoperative treatment? *Cancer* 2012;118(2):392–403.
75. Grigsby PW, Siegel BA, Dehdashti F. Lymph node staging by positron emission tomography in patients with carcinoma of the cervix. *J Clin Oncol* 2001;19(17):3745–9.

76. Kidd EA, Siegel BA, Dehdashti F, et al. Lymph node staging by positron emission tomography in cervical cancer: relationship to prognosis. *J Clin Oncol* 2010;28(12):2108–13.
77. Kidd EA, Siegel BA, Dehdashti F, et al. Pelvic lymph node F-18 fluorodeoxyglucose uptake as a prognostic biomarker in newly diagnosed patients with locally advanced cervical cancer. *Cancer* 2010;116(6):1469–75.
78. Pan L, Cheng J, Zhou M, et al. The SUVmax (maximum standardized uptake value for F-18 fluorodeoxyglucose) and serum squamous cell carcinoma antigen (SCC-ag) function as prognostic biomarkers in patients with primary cervical cancer. *J Cancer Res Clin Oncol* 2012;138(2):239–46.
79. Viswanathan C, Faria S, Devine C, et al. [18F]-2-Fluoro-2-Deoxy-D-glucose-PET Assessment of Cervical Cancer. *PET Clin* 2018;13(2):165–77.
80. Chung HH, Kim SK, Kim TH, et al. Clinical impact of FDG-PET imaging in post-therapy surveillance of uterine cervical cancer: from diagnosis to prognosis. *Gynecol Oncol* 2006;103(1):165–70.
81. Cetina L, Serrano A, Cantú-de-León D, et al. F18-FDG-PET/CT in the evaluation of patients with suspected recurrent or persistent locally advanced cervical carcinoma. *Rev Invest Clin* 2011;63(3):227–35.
82. Grigsby PW, Siegel BA, Dehdashti F, et al. Posttherapy surveillance monitoring of cervical cancer by FDG-PET. *Int J Radiat Oncol Biol Phys* 2003;55(4):907–13.
83. Siva S, Herschtal A, Thomas JM, et al. Impact of post-therapy positron emission tomography on prognostic stratification and surveillance after chemoradiotherapy for cervical cancer. *Cancer* 2011;117(17):3981–8.
84. Schwartz M, Gavane SC, Bou-Ayache J, et al. Feasibility and diagnostic performance of hybrid PET/MRI compared with PET/CT for gynecological malignancies: a prospective pilot study. *Abdom Radiol (Ny)* 2018;43(12):3462–7.
85. Grueneisen J, Schaarschmidt BM, Heubner M, et al. Integrated PET/MRI for whole-body staging of patients with primary cervical cancer: preliminary results. *Eur J Nucl Med Mol Imaging* 2015;42(12):1814–24.
86. Gong J, Wang N, Bian L, et al. Cervical cancer evaluated with integrated 18F-FDG PET/MR. *Oncol Lett* 2019;18(2):1815–23.
87. Surov A, Meyer HJ, Schob S, et al. Parameters of simultaneous 18F-FDG-PET/MRI predict tumor stage and several histopathological features in uterine cervical cancer. *Oncotarget* 2017;8(17):28285–96.
88. Shih IL, Yen RF, Chen CA, et al. PET/MRI in Cervical Cancer: Associations Between Imaging Biomarkers and Tumor Stage, Disease Progression, and Overall Survival. *J Magn Reson Imaging* 2021;53(1):305–18.
89. Abu-Rustum NR, Lee S, Correa A, et al. Compliance with and acute hematologic toxic effects of chemoradiation in indigent women with cervical cancer. *Gynecol Oncol* 2001;81(1):88–91.
90. Torres MA, Jhingran A, Thames HD, et al. Comparison of treatment tolerance and outcomes in patients with cervical cancer treated with concurrent chemoradiotherapy in a prospective randomized trial or with standard treatment. *Int J Radiat Oncol Biol Phys* 2008;70(1):118–25.
91. Wyss JC, Carmona R, Karunamuni RA, et al. [(18F)] Fluoro-2-deoxy-2-d-glucose versus 3'-deoxy-3'-[(18F)]fluorothymidine for defining hematopoietically active pelvic bone marrow in gynecologic patients. *Radiother Oncol* 2016;118(1):72–8.
92. Grigsby PW, Malyapa RS, Higashikubo R, et al. Comparison of molecular markers of hypoxia and imaging with (60)Cu-ATSM in cancer of the uterine cervix. *Mol Imaging Biol* 2007;9(5):278–83.
93. Adams TS, Cuello MA. Cancer of the vagina. *Int J Gynaecol Obstet* 2018;143(Suppl 2):14–21.
94. Lamoreaux WT, Grigsby PW, Dehdashti F, et al. FDG-PET evaluation of vaginal carcinoma. *Int J Radiat Oncol Biol Phys* 2005;62(3):733–7.
95. Robertson NL, Hricak H, Sonoda Y, et al. The impact of FDG-PET/CT in the management of patients with vulvar and vaginal cancer. *Gynecol Oncol* 2016;140(3):420–4.
96. Koh WJ, Greer BE, Abu-Rustum NR, et al. Vulvar Cancer, Version 1.2017, NCCN Clinical Practice Guidelines in Oncology. *J Natl Compr Cancer Netw* 2017;15(1):92–120.
97. Peiró V, Chiva L, González A, et al. [Utility of the PET/CT in vulvar cancer management]. *Rev Esp Med Nucl Imagen Mol* 2014;33(2):87–92.
98. Cohn DE, Dehdashti F, Gibb RK, et al. Prospective evaluation of positron emission tomography for the detection of groin node metastases from vulvar cancer. *Gynecol Oncol* 2002;85(1):179–84.
99. Kamran MW, O'Toole F, Meghen K, et al. Whole-body [18F]fluoro-2-deoxyglucose positron emission tomography scan as combined PET-CT staging prior to planned radical vulvectomy and inguinofemoral lymphadenectomy for squamous vulvar cancer: a correlation with groin node metastasis. *Eur J Gynaecol Oncol* 2014;35(3):230–5.
100. Viswanathan C, Kirschner K, Truong M, et al. Multimodality imaging of vulvar cancer: staging, therapeutic response, and complications. *AJR Am J Roentgenol* 2013;200(6):1387–400.
101. Lin G, Chen CY, Liu FY, et al. Computed tomography, magnetic resonance imaging and FDG positron emission tomography in the management of

- vulvar malignancies. *Eur Radiol* 2015;25(5):1267–78.
102. Antunes P, Ginj M, Zhang H, et al. Are radiogallium-labelled DOTA-conjugated somatostatin analogues superior to those labelled with other radiometals? *Eur J Nucl Med Mol Imaging* 2007;34(7):982–93.
  103. Virgolini I, Ambrosini V, Bomanji JB, et al. Procedure guidelines for PET/CT tumour imaging with 68Ga-DOTA-conjugated peptides: 68Ga-DOTA-TOC, 68Ga-DOTA-NOC, 68Ga-DOTA-TATE. *Eur J Nucl Med Mol Imaging* 2013;37(10):2004–10.
  104. Miller B, Dockter M, el Torky M, et al. Small cell carcinoma of the cervix: a clinical and flow-cytometric study. *Gynecol Oncol* 1991;42(1):27–33.
  105. Damian A, Lago G, Rossi S, et al. Early Detection of Bone Metastasis in Small Cell Neuroendocrine Carcinoma of the Cervix by 68Ga-DOTATATE PET/CT Imaging. *Clin Nucl Med* 2017;42(3):216–7.
  106. Delpassand ES, Ranganathan D, Wagh N, et al. 64Cu-DOTATATE PET/CT for Imaging Patients with Known or Suspected Somatostatin Receptor-Positive Neuroendocrine Tumors: Results of the First U.S. Prospective, Reader-Masked Clinical Trial. *J Nucl Med* 2020;61(6):890–6.
  107. Neve RM, Lane HA, Hynes NE. The role of overexpressed HER2 in transformation. *Ann Oncol* 2001;12(Suppl 1):S9–13.
  108. Bensch F, Lamberts LE, Smeenk MM, et al. 89Zr-Lumretuzumab PET Imaging before and during HER3 Antibody Lumretuzumab Treatment in Patients with Solid Tumors. *Clin Cancer Res* 2017;23(20):6128–37.
  109. Chan CY, Tan KV, Cornelissen B. PARP Inhibitors in Cancer Diagnosis and Therapy. *Clin Cancer Res* 2020;10:1585–94.
  110. Makvandi M, Pantel A, Schwartz L, et al. A PET imaging agent for evaluating PARP-1 expression in ovarian cancer. *J Clin Invest* 2018;128(5):2116–26.
  111. Richard SD, Bencherif B, Edwards RP, et al. Noninvasive assessment of cell proliferation in ovarian cancer using [18F] 3'deoxy-3-fluorothymidine positron emission tomography/computed tomography imaging. *Nucl Med Biol* 2011;38(4):485–91.
  112. Tsuyoshi H, Morishita F, Orisaka M, et al. 18F-fluorothymidine PET is a potential predictive imaging biomarker of the response to gemcitabine-based chemotherapeutic treatment for recurrent ovarian cancer: preliminary results in three patients. *Clin Nucl Med* 2013;38(7):560–3.
  113. Aide N, Kinross K, Cullinane C, et al. 18F-FLT PET as a surrogate marker of drug efficacy during mTOR inhibition by everolimus in a preclinical cisplatin-resistant ovarian tumor model. *J Nucl Med* 2010;51(10):1559–64.